Article

Not peer-reviewed version

Neutralization and Binding Capability of SARS-CoV-2 Variants by/of IgG Antibodies of Early COVID-19 Convalescent Inactivated Sera based on Indirect ELISA

Behzad Hussain , Peizhe Zhao , Bo Yang , Xiaoxiong Li , Zhichao Zhang , Guoqiang Feng , Demei Zhang * , Defen Lu * , Changxin Wu *

Posted Date: 21 May 2024

doi: 10.20944/preprints202405.1313.v1

Keywords: SARS-CoV-2; neutralization; early COVID-19; convalescent sera; ELISA

Article

Neutralization and Binding Capability of SARS-CoV-2 Variants by/of IgG Antibodies of Early COVID-19 Convalescent Inactivated Sera Based on Indirect ELISA

Behzad Hussain [1], Peizhe Zhao [2], Bo Yang [3], Xiaoxiong Li [3], Zhichao Zhang [3], Guoqiang Feng [2], Demei Zhang [2,*], Defen Lu [4,*] and Wu Changxin [1,*]

[1] Institutes of Biomedical Sciences, Shanxi University, Taiyuan, China
[2] Department of Blood Transfusion, Taiyuan Blood Centre, Taiyuan, China
[3] Shanxi Academy of Advanced Research and Innovation, Taiyuan, China
[4] College of Life Sciences, Shanxi Agricultural University, Taiyuan, China
* Correspondence: 13834532717@126.com (D.Z.); ludefen1@sxau.edn.cn (D.L.); cxw20@sxu.edu.cn (W.C.)

Abstract: Severe Acute Respiratory Syndrome Coronavirus 2 (SARS-CoV-2) is a single stranded RNA virus which has resulted in the Coronavirus Disease 2019 (COVID-19) pandemic and has infected millions of people all over the world. SARS-CoV-2 has been mutating rapidly resulting in the emergence of multiple variants to escape the host immune system mainly by mutations in its receptor binding domain (RBD) of the spike protein. This rapid evolution of the SARS-CoV-2 posed a great challenge regarding the efficacy and effectiveness of the current SARS-CoV-2 vaccines. The RBD and full-length spike of SARS-CoV-2 is the main target of the neutralizing antibodies. Many SARS-CoV-2 variants are considered to have the potential to escape from the host immune system. In this study, the RBD of Alpha, Beta, Gamma, Kappa and Omicron and the full-length spike of BA.1, BA.2, BA.3, BA.4/5, BQ.1.1 and XBB.1.5 Omicron variants were used as coating antigens in Enzyme Linked Immuno-Sorbent Assay (ELISA) to check the neutralization capability of COVID-19 convalescent sera from patients of first wave of infection occurring in Wuhan. Our results show that the currently circulating Omicron BQ.1.1, XBB.1.5 and previous Omicron BA.1, BA.2 and BA.4/5 do not show significant reduction in neutralization, while Omicron BA.3 and previous variants Alpha, Beta, Gamma, Kappa, and Omicron showed a significantly reduced neutralization when compared to the wild-type Wuhan strain. These results indicate patients recovering from natural infection of early original Wuhan strain may have the potential to resist infection of current circulating variants and the vaccines using the prototype antigen may still working for newly emerged variants.

Keywords: SARS-CoV-2; neutralization; early COVID-19; convalescent sera; ELISA

1. Introduction

The severe acute respiratory syndrome coronavirus 2 (SARS-CoV-2) emerged in Wuhan City, People's Republic of China in December 2019 causing coronavirus disease 2019 (COVID-19), that was declared as a global pandemic in March 2020 [1]. The disease has infected a total of 771.5497 million people globally with deaths of 6.9744 million as of October 25, 2023. A total number of 13.5164 billion vaccine doses have been administered as of October 15, 2023 (https://covid19.who.int/).

The SARS-CoV-2 is a positive-sense RNA containing virus with an envelope outside. It enters the target host cells via its spike (S) protein. The spike is the most important protein to start the virus infection of host cells and it is the most immunogenic proteins in comparison to the other viral proteins [2]. The antibodies of the infecting host prevent the binding and entry of the virus into the

 doi:10.20944/preprints202405.1313.v1

host cell by neutralizing the viral spike protein. The virus helps to escape from the host immune system by mutating at a very high rate and reducing the antibody binding activity or neutralizing capability. This reduces the effectiveness of the antibodies production by natural infection as well as the vaccines targeting the spike protein as most of the anti-SARS-CoV-2 vaccines target the viral spike protein [3].

Within the spike, the RBD binds with the human cell receptor angiotensin converting enzyme 2 (ACE-2) to enter the cell. Both the RBD and full-length spike proteins have been used in serological assays like enzyme linked immunosorbent assay (ELISA) [4–6].

While SARS-CoV-2 possesses a proofreading mechanism (NSP14), it has still been mutating at a relatively high rate, as studied by Gribble et al. (2021). resulting in the emergence of new variants [7,8]. For instance, the Alpha (B.1.1.7), Beta (B.1.351), Delta (B.1.617.2), Gamma (P.1), Kappa (B.1.617.1) and Omicron (B.1.1.529) are some of the key variants with a higher rate of mutation compared to the original Wuhan strain of SARS-CoV-2 . The Omicron lineage has many sub-lineages for example BA.1 (previously known as B.1.1.529), BA.2, BA.3, BA.4/5, BQ.1.1 and XBB.1.5 etc. [9].

The Alpha, Beta, Gamma, Delta and Kappa variants are now classified as the variants being monitored (VBM) being no longer detected, suggesting that these are now circulating at very low, undetectable levels or might have been outcompeted by more rapidly transmissible variants while the Omicron variants are still the variants of concern (VOC) meaning that some sub-lineages of Omicron lineage still show significant reduction in the neutralization by serum antibodies produced during the prior infection or vaccination [10,11].

The presence of multiple mutations in the viral spike questions the efficacy of SARS-CoV-2 vaccines and there is a need to study whether the currently circulating variants of SARS-CoV-2 can be neutralized by antibodies generated from the original or wild-type Wuhan strain. Hence, in this study, the neutralization activity and binding capability of RBD of wild-type, Alpha (N501Y mutation), Beta (K417N/E484K/N501Y mutations), Gamma (K417E/E484K/N501Y mutations), Kappa (L452R/E484Q mutations) and Omicron BA.1 (T547K mutation) variants and full-length spike of SARS-CoV-2 wild-type and BA.1, BA.2, BA.2.12.1, BA.3, BA.4/5, BQ.1.1 and XBB.1.5 Omicron variants by/of serum IgG antibodies of the early COVID-19 convalescent sera was checked using these proteins as coating antigens in an indirect ELISA assay. This study first checked the neutralizing activity and binding capability by measuring the OD450nm values, then the S/N ratios of each respective variant and then the reduction rates (%) for all the variants. This study will help in making decisions to update the anti-SARS-CoV-2 vaccine design against the newly circulating variants based on their immune evasion.

2. Materials and Methods

Sample Collection and Cryopreservation

A total of 65 SARS-CoV-2 Wuhan strain convalescent serum samples were taken/collected from the Department of Blood Transfusion, Taiyuan Blood Center, Taiyuan, Shanxi province, People's Republic of China from January to May 2020, transported to the laboratory under cold chain and stored at -80°C until further processing. The presence and absence of SARS-CoV-2 infection was first checked/screened by Diagnostic Kit for SARS-CoV-2 IgM Antibody (ELISA) (Shanghai Kehua Bio-engineering Co., Ltd. (KHB®), P.R. China) which targeted the nucleocapsid (N) gene of the SARS-CoV-2 genomeand confirmed by Diagnostic kit for SARS-CoV-2 Nucleic Acid (Real Time PCR) (Shanghai Kehua Bio-engineering Co., Ltd. (KHB®), P.R. China) which targeted ORF1ab/N/E genes of the SARS-CoV-2 genome from the nasopharyngeal fluid swabs. The sera were inactivated by heating at 37°C for 30 minutes. The study was approved by the ethical committee of Shanxi University, China.

 doi:10.20944/preprints202405.1313.v1

Cloning and Expression Clones

For the SARS-CoV-2 wild type, Alpha, Beta, Gamma, Kappa and Omicron variants, the DNA encoding for the respective receptor binding domains and for the SARS-CoV-2 wild type and the BA.1, BA.2, BA.3, BA.4/5, BQ.1.1 and XBB.1.5 Omicron variants, full-length spike were cloned into the pCAGGS mammalian expression vector by Gibson Assembly cloning method and the clones were sequence confirmed by the Sanger's sequencing. pCAGGS vector was first enzymatically digested with EcoR-I/Xho-I restriction enzymes followed by ligation of the PCR-amplified and gel-purified RBDs (amino acid position 319 to 541; numbering is according to the RBD of wild-type Wuhan strain) and full-length spikes (amino acid position 576 to 1853; numbering is according to the full-length spike of wild-type Wuhan strain) of each respective variant by Gibson clone system according to manufacturer's protocol with some modifications. The recombinant plasmids were then transformed into the competent bacterial cells (E. coli TOP10-200715; Tiangen Biotech (Beijing) Co., Ltd., P.R. China) by heat-shock method. The successfully transformed E.coli cells were then outgrown in LB broth for overnight followed by isolation of the recombinant vector carrying the respective target protein by EndoFree Maxi Plasmid Kit DP-117; Tiangen Biotech) Beijing) Co. Ltd., P.R. China) according to the manufacturer's instructions with some modifications and checked the concentration (ng/µL) and purity (A280/A260 and A260/A230 ratios) of the isolated/purified plasmids by Nanodrop Spectrophotometer (ThermoFisher ScientificTM). The purified recombinant plasmid vectors were stored at -20°C until further processing. All the clones had 6X-His-tag at their C-terminal end for purification of the expressed proteins.

Protein Expression

Human Embryonic Kidney (HEK)-293F suspension cells (FreeStyleTM 293-F cells; ThermoFisher ScientificTM) were cultured into their respective shaker flasks containing SMM293-TII cell culture medium (SinoBiological Inc. P.R. China). Transient transfection of the cells with the purified recombinant pCAGGS expression plasmid vectors was done using PEI (polyethylenimine) transfection method with plasmid to PEI ratio of 1:3. Sodium chloride (NaCl-300mM) was used as a transfection buffer. After 24 hours of incubation of cells with the plasmid, sodium valproate salt and sodium valproic acid were added as feed solution to enhance the expression. The cells were incubated for a total of 7 days after which protein purification was performed.

Protein Purification

After 7 days of incubation, the cells were processed for protein purification by nickel affinity column chromatography and size exclusion chromatography according to the optimized protocol.

After pelleting down the cells, pH of the supernatant was adjusted to 8.0 by 1M Tris-HCl (pH = 8.0) and filtered by 0.22µm filter paper using the water-circulation multifunction vacuum pump (Zhengzhou Greatwall Scientific Industrial and Trade Co., Ltd., P.R. China). Proteins smaller than 50KDa size were filtered out using Vivaflow50/50R/200 machine (Sartorius Stedim Lab Ltd., UK) using 50KDa filter membrane using buffer A (20mM Tris-HCl, 500mM NaCl, 10mM Imidazole, pH 8.0) as per the manufacturer's protocol.

The histidine-tagged proteins were then purified by the nickel affinity column chromatography by passing the filtrate through nickel affinity gravity column (20mL; EasyBio; 7321010-5) with nickel sepharose (6 Fast Flow soltution; Cytiva Life Sciences) using buffer A (10CV) as washing buffer and buffer B-8ml (20mM Tris-HCl, 500mM NaCl, 250mM Imidazole, pH 8.0) as elution buffer. The eluate was then concentrated concentration tube (50,000 Molecular Weight Cut-Off-MWCO Amicon® Ultra-15 Centrifugal Filter Units by MerckMillipore) by centrifugation at 2300xg speed (not more) on the KDC-2044 Low Speed Refrigerated Centrifuge (Anhui USTC Zonkia Scientific Instruments Co. Ltd., P.R. China) followed by sodium dodecyl sulphate-polyacrylamide gel electrophoresis (SDS-PAGE) and Coomassie brilliant blue (CBB) staining.

Size exclusion chromatography was performed by fast protein liquid chromatography (FPLC) using the AKTA pure machine (GE Healthcare; Cytiva) using SuperoseTM 6 Increase 10/300 GL

 doi:10.20944/preprints202405.1313.v1

and/or SuperdexTM 200 Increase 10/300 GL GE Healthcare columns as per manufacturer's protocol with some modifications. The concentrated protein sample was run at 0.4ml/min flow rate and fractions were collected by the Fraction Collector F9-R. The fractions were then checked for the presence and purity of the target protein using SDS-PAGE followed by CBB staining.

To quantify the purified proteins, spectrophotometry using a Nanodrop machine was used to measure the absorbance at 280nm wavelength. The absorbance values were then converted into the actual concentration of the respective proteins based on their extinction coefficients. The purified proteins were checked for their purity by SDS-PAGE and CBB staining (Coomassie brilliant blue R-250-1mg/mL in MeOH; Solarbio® Life Sciences) using 10-12% denaturing SDS-PAGE gel (acrylamide/bisacrylamide in 1:29 ratio) containing Dithiothreitol (DTT). The sizes of the proteins were compared with 180KDa PageRulerTM Prestained Protein Ladder (ThermoFisher ScientificTM). The results were also confirmed by Western blot analysis using anti-His and anti-GAPDH antibodies (Proteintech® company). The purified proteins were then coated on ELISA plates as coating antigens and tested against the SARS-CoV-2 Wuhan convalescent sera.

Indirect Enzyme Linked Immunosorbent Assay (iELISA)

96 well EIA/RIA plates (Corning™ Costar® USA #3590) were coated with 100ng/well of the purified proteins. The positive and negative controls were coated at 10µg/well. The coating was performed at 4°C for 6-8 hours in the 1X ELISA coating buffer (Solarbio® Life Sciences) followed by blocking the wells with 100µL/well of 8% skim milk powder (Beyotime Biotechnology company) prepared in 1X phosphate buffered saline containing 0.5% Tween-20 (PBST) for overnight at 4°C and washing thrice with 1X PBST. Serum samples were diluted at 1:80 ratio in 8% skimmed milk, added 100µL/well, incubated in a 37°C incubator for 1 hour, washed the wells of the plate with 150µL/well 1X PBST thrice, detected the binding antibody using 1:10,000 diluted 100µL/well (prepared in 8% skimmed milk) Goat Anti-Human IgG antibodies conjugated with horseradish peroxidase-HRP enzyme) (OriGene Technologies, Inc. and/or ABclonal company) and incubated in a 37°C incubator for 1 hour. The wells were then washed with 150µL/well 1X PBST thrice, added 50µL/well chromogen/HRP substrate TMB HRP Color Development Solution for ELISA (Beyotime company), incubated for 2-3 minutes in dark at room temperature and added 50µL/well ELISA Stop solution (Solarbio® Life Sciences) to stop the enzymatic reaction. The Optical Density (O.D.) at 450nm wavelength was then measured on BioTek ELx800 (Gene Company Limited) ELISA plate reader and the results were then analyzed by GraphPad Prism 9.5.1 software. The samples and the positive and negative control were run in triplicates.

Statistical Analysis

The neutralizing activity and binding capability of the RBD of Alpha, Beta, Gamma, Kappa, and Omicron BA.1 and the full-length spike of BA.1, BA.2, BA.3, BA.4/5, BQ.1.1 and XBB.1.5 Omicron SARS-CoV-2 variants to the convalescent sera of SARS-CoV-2 original Wuhan strain was determined by analyzing the data of OD450nm values and by calculating the S/N ratios of the OD450nm values for each respective variant respectively using the GraphPad Prism 9.5.1 software.

The S/N ratios were calculated using the following formula:

S/N* ratio = (OD450nm value of the SARS-CoV-2 Convalescent sera)/(OD450nm value of the PCR-negative control)

*S = Signal; N = Noise

The purified proteins of the respective variants of the SARS-CoV-2 were coated onto the 96-well ELISA plates as coating antigens followed by ELISA assay. The OD450nm values of the ELISA assay were then analyzed by appropriate statistical tests using GraphPad Prism version 9.5.1 software. A p-value of < 0.05 was considered statistically significant. Statistical significance was noted as follows: * $p < 0.05$, ** $p < 0.01$, *** $p < 0.001$ and **** $p < 0.0001$. Error bars in terms of either Mean ± standard deviation (SD) and/or Mean ± standard error of mean (SEM) were shown.

The reduction in binding (i.e., the reduction rate) was calculated using the following formula:

 doi:10.20944/preprints202405.1313.v1

Reduction rate = ((OD450nm of RBD or Spike of WT strain-OD450nm of the variant))/(OD450nm of WT strain) × 100

The OD450nm values were normalized by subtracting each of the OD450nm values of the serum sample from those of the blank wells. The data was analyzed by GraphPad Prism version 9.5.1 software. As the software does not analyze the data if a negative value is present so the negative values were removed from the datasets, if any before analyzing the data.

3. Results

3.1. Sample Collection and Cryopreservation

A total of 65 COVID-19 convalescent serum samples were used in this study which were collected from the unvaccinated individuals during the initial phase of COVID-19 outbreak in 2020. The sera were collected by the Department of Blood Transfusion, Taiyuan Blood Center, Taiyuan, Shanxi province, P.R. China. Out of 65 sera, 51 were SARS-CoV-2 PCR positive and 14 were PCR negative. Most of the PCR positive sera were from Yuncheng (n=32) followed by Jinzhong (n=5), Taiyuan (n=3), Datong (n=2), Lvliang (n=2), Changzhi (n=2), Xinzhou (n=2), Jincheng (n=1), Pingyao (n=1) and Shuozhou (n=1). The PCR negative sera were used as negative control to calculate the S/N ratios. The demographic details including the sample collection date, city name, blood type, gender, age and PCR status of the convalescents have been provided in Table 1.

Table 1. Details of the serum samples used in this study.

Sr. No.	Sample ID	Sample Collection Date	Demographic Location (City)	Blood type	Gender	Age (years)	PCR* status (-ve or +ve)
1	Y1	18-02-2020	Yuncheng	O	Male	27	+ve
2	Y2	11-05-2020	Yuncheng	B	Female	24	+ve
3	Y3	26-04-2020	Yuncheng	O	Male	27	+ve
4	Y4	29-01-2020	Yuncheng	A	Male	23	+ve
5	Y5	22-02-2020	Yuncheng	A	Male	32	+ve
6	Y6	03-03-2020	Yuncheng	O	Male	27	+ve
7	Y7	19-03-2020	Yuncheng	B	Female	22	+ve
8	Y8	19-03-2020	Yuncheng	A	Male	32	+ve
9	Y9	23-01-2020	Yuncheng	B	Female	22	+ve
10	Y10	02-05-2020	Yuncheng	AB	Male	35	+ve
11	Y11	19-03-2020	Yuncheng	O	Male	27	+ve
12	Y12	19-03-2020	Yuncheng	B	Male	38	+ve
13	Y13	09-02-2020	Yuncheng	B	Male	28	+ve
14	Y14	18-02-2020	Yuncheng	AB	Male	38	+ve
15	Y15	03-05-2020	Yuncheng	O	Male	27	+ve
16	Y16	19-03-2020	Yuncheng	O	Female	26	+ve
17	Y17	19-03-2020	Yuncheng	O	Male	32	+ve
18	Y18	18-02-2020	Yuncheng	A	Male	32	+ve
19	Y19	20-02-2020	Yuncheng	O	Male	27	+ve
20	Y20	19-03-2020	Yuncheng	A	Male	45	+ve
21	Y21	10-04-2020	Yuncheng	O	Male	27	+ve
22	Y22	02-05-2020	Yuncheng	A	Male	23	+ve
23	Y23	10-02-2020	Yuncheng	A	Male	45	+ve
24	Y24	19-03-2020	Yuncheng	B	Male	43	+ve
25	Y25	19-03-2020	Yuncheng	O	Male	39	+ve
26	Y26	19-03-2020	Yuncheng	A	Male	37	+ve
27	Y27	19-03-2020	Yuncheng	O	Female	26	+ve

 doi:10.20944/preprints202405.1313.v1

28	Y28	19-03-2020	Yuncheng	AB	Male	26	+ve
29	22	02-05-2020	Datong	B	Male	25	+ve
30	32	02-05-2020	Yuncheng	A	Male	45	+ve
31	34	02-05-2020	Luliang	A	Male	28	+ve
32	434	02-05-2020	Jinzhong	AB	Male	32	+ve
33	A20	02-05-2020	Taiyuan	O	Female	40	+ve
34	1048	02-05-2020	Xinzhou	A	Female	38	+ve
35	1090	02-05-2020	Xinzhou	B	Male	43	+ve
36	1092	02-05-2020	Pingyao	AB	Male	26	+ve
37	1094	02-05-2020	Jinzhong	O	Male	32	+ve
38	1096	02-05-2020	Yuncheng	AB	Male	35	+ve
39	1435	02-05-2020	Jinzhong	O	Male	21	+ve
40	1443	02-05-2020	Datong	B	Male	25	+ve
41	1444	02-05-2020	Jinzhong	O	Male	27	+ve
42	2234	02-05-2020	Changzhi	B	Male	27	+ve
43	2237	02-05-2020	Yuncheng	AB	Male	26	+ve
44	2255	02-05-2020	Jincheng	A	Female	44	+ve
45	2256	02-05-2020	Shuozhou	A	Male	30	+ve
46	2494	02-05-2020	Yuncheng	O	Male	39	+ve
47	2497	02-05-2020	Taiyuan	B	Male	42	+ve
48	2506	02-05-2020	Jinzhong	O	Male	49	+ve
49	2601	02-05-2020	Luliang	A	Male	28	+ve
50	2602	02-05-2020	Changzhi	AB	Female	23	+ve
51	2604	02-05-2020	Taiyuan	A	Male	35	+ve
52	2080	02-05-2020	Taiyuan	O	Male	31	-ve
53	2081	02-05-2020	Taiyuan	**O**	**Male**	**35**	-ve
54	2082	02-05-2020	Taiyuan	**B**	**Male**	**28**	-ve
55	2083	02-05-2020	Taiyuan	**AB**	**Male**	**38**	-ve
56	2084	02-05-2020	Taiyuan	**B**	**Male**	**30**	-ve
57	2085	02-05-2020	Taiyuan	**A**	**Male**	**44**	-ve
58	2086	02-05-2020	Taiyuan	**A**	**Male**	**27**	-ve
59	2087	02-05-2020	Taiyuan	**O**	**Male**	**40**	-ve
60	2088	02-05-2020	Taiyuan	**AB**	**Male**	**37**	-ve
61	2089	02-05-2020	Taiyuan	**AB**	**Male**	**26**	-ve
62	2090	02-05-2020	Taiyuan	**O**	**Male**	**28**	-ve
63	2092	02-05-2020	Yangquan	B	Male	38	-ve
64	2093	02-05-2020	Jinzhong	O	Male	49	-ve
65	2094	02-05-2020	Jincheng	A	Female	28	-ve

3.2. Binding Capability of RBD and Full-Length Spike

The RBD and full-length spike proteins of different variants of the SARS-CoV-2 (Table 2) were expressed using mammalian suspension culture. The proteins were purified using nickel affinity column chromatography, followed by size exclusion chromatography, SDS-PAGE and CBB staining (Supplementary Figure S1A–J). The purified proteins were then used as coating antigens in the 96-well ELISA plates for checking the neutralization and binding capability of RBD and full-length spike from SARS-CoV-2 variants to the SARS-CoV-2 Wuhan convalescent sera.

The data of normalized OD450nm values of full-length spike of the wild-type SARS-CoV-2 and Omicron variants was analyzed by the Brown-Forsythe and Welch's ANOVA with Dunnett's T3 multiple comparison statistical test.

 doi:10.20944/preprints202405.1313.v1

Table 2. The SARS-CoV-2 variants used in this study.

Variant Name (As per WHO)	Other Names	Key RBD/Spike/other mutation (s)	First time detected in	First time detected from	Reference
Alpha	B.1.1.7, 20I/501Y.V1, GRY, VOC 202012/01	N501Y, A570D, P681H, T716I, S982A and D1118H	2020	United Kingdom	[29]
Beta	B.1.351, GH, 20H/501Y.V2,	RBD: K417N, E484K and N501Y	2020	South Africa	[29]
Gamma	P.1, B.1.1.28.1, GR, 20J/501Y.V3	K417T, E484K and N501Y	2020	Brazil	[30]
Kappa	B.1.617.1, 21B, G/452R.V3, 20A/S:154K	L452R and E484Q	2021	India	[30]
Omicron	B.1.1529, 21K, 21L, 21M, GR/484A	G339D, S371L, S373P, S375F, K417N, N440K, G446S, S477N, T478K, E484A, Q493R, G496S, Q498R, N501Y and Y505H	2021	Botswana	[31,32]
Omicron BA.1	B.1.1.529.1	T547K	2021	South Africa	[33]
Omicron BA.2	B.1.1.529.2	V213G	2021	South Africa	[33]
Omicron BA.3	B.1.1.529.3	No unique RBD or spike mutation. Others: C832T and C11235T	2021	South Africa	[33]
Omicron BA.4/5	B.1.1.529.4/5	69-70del, L452R, and F486V; Others: N: P151S, ORF7b: L11F, and NSP1:141-143del	2022	South Africa	[34,35]
Omicron BQ.1.1	B.1.1.529.5.3.1.1.1.1.1.1	ORF1b: N1191S and S: R346T, N460K	2022	Nigeria	[36]
Omicron XBB.1.5	23A	S: F486P	2022	United States of America	[37]

Table 2. The SARS-CoV-2 variants used in this study.

Sample ID	Wild-type	Alpha	Beta	Gamma	Kappa	Omicron BA.1	Alpha	Beta	Gamma	Kappa	Omicron BA.1
	Normalized OD450nm						% Reduction rate				
Y1	0.5906					0.0217					96.3241
Y3	0.5516					0.0327					94.0699
Y6	0.6169					0.0260					95.7786
Y11	0.6216					0.0387					93.7724
Y14	0.0772					0.0080					89.5870
Y17	0.0712	0.0185	0.0429	0.0633	0.0499	0.0767	74.0250	39.7036	11.0764	29.8947	-7.7028
Y18	0.6452					0.0244					96.2223
Y20	0.4822	0.0825	0.2151	0.2907	0.2029	0.1307	82.8917	55.3917	39.7235	57.9176	72.8946
434	0.0743	0.0365	0.0627	0.0598	0.0564	0.0697	50.8754	15.7011	19.5872	24.1833	6.2286
A20	0.0372	0.0200	0.0358	0.0320	0.0307	0.0364	46.3758	3.8943	14.0421	17.5490	2.2900
32	0.4472	0.0708	0.2168	0.2827	0.1998		84.1615	51.5280	36.7950	55.3323	
22	0.3422	0.1392	0.1734	0.2278	0.1814	0.0809	59.3188	49.3190	33.4264	46.9854	76.3518
1048	0.3469	0.0649	0.1329	0.1356	0.1050	0.0818	81.3050	61.6918	60.9231	69.7234	76.4137
1090	0.5393	0.1511	0.4273	0.3681	0.2831	0.1146	71.9890	20.7672	31.7477	47.5026	78.7523
1092	0.6090	0.2219	0.4743	0.3924	0.3439	0.1232	63.5714	22.1134	35.5598	43.5281	79.7780
1094	0.3238	0.0967	0.1162	0.1201	0.1000	0.0527	70.1217	64.1049	62.9038	69.1065	83.7211
1096	0.1120	0.0302	0.0557	0.0780	0.0618	0.0675	73.0502	50.3000	30.3604	44.8563	39.7474
1435	0.6398	0.2261	0.5523	0.5703	0.4649	0.1504	64.6668	13.6773	10.8552	27.3300	76.4959
1443	0.4051	0.0876	0.1973	0.2662	0.1593	0.0928	78.3876	51.3034	34.2987	60.6869	77.0882
1444	0.6337	0.1072	0.2221	0.2755	0.1893	0.1025	83.0806	64.9513	56.5267	70.1346	83.8257
2234	0.2787	0.0811	0.1219	0.1707	0.1423	0.0763	70.9189	56.2687	38.7682	48.9585	72.6131
2237	0.7146	0.2917	0.4901	0.5675	0.4804	0.1592	59.1743	31.4104	20.5800	32.7651	77.7251
2255	0.5131	0.1106	0.1944	0.2577	0.2131	0.0825	78.4515	62.1007	49.7780	58.4651	83.9226
2256	0.2202	0.0345	0.0851	0.1022	0.0756	0.0652	84.3262	61.3536	53.6091	65.6735	70.4161
2494	0.3659	0.0601	0.1266	0.1683	0.1196	0.0843	83.5864	65.3963	53.9933	67.3132	76.9511
2497	0.7069	0.1897	0.4673	0.5163	0.4076	0.1543	73.1610	33.8966	26.9569	42.3393	78.1672
2506	0.4711	0.0977	0.2163	0.2747	0.1899	0.0740	79.2546	54.0866	41.6912	59.6798	84.2906
2601	0.2567	0.0452	0.0868	0.1167	0.0849	0.0612	82.3848	66.1978	54.5553	66.9173	76.1740
2602	0.3916	0.0919	0.1969	0.2517	0.1704	0.1588	76.5323	49.7020	35.7264	56.4735	59.4353
2604	0.5237	0.1294	0.3768	0.4072	0.3023	0.1483	75.2944	28.0577	22.2552	42.2855	71.6771

 doi:10.20944/preprints202405.1313.v1

We evaluated the ability of SARS-CoV-2 Alpha (N501Y single mutation), Beta (K417N, E484K and N501Y mutations), Gamma (K417E, E484K and N501Y mutations), Kappa (L452R and E484Q double mutation), and Omicron (BA.1, BA.2, BA.3, BA.4/5, BQ.1.1 and XBB.1.5) variants to escape antibodies induced by natural infection of original Wuhan strain of SARS-CoV-2 using the indirect ELISA method. The Alpha, Beta, Gamma, Kappa and Omicron BA.1 variants were evaluated based on their RBDs while the BA.1, BA.2, BA.3, BA.4/5, BQ.1.1 and XBB.1.5 Omicron variants were evaluated based on their full-length spike proteins.

We found that the Omicron variant had significantly lowest OD450nm values followed by Alpha, Kappa, Beta, and Gamma variants based on their RBDs which means that the Omicron BA.1 has the least binding and neutralizing capability/activity followed by Alpha, Kappa, Beta, and Gamma variants and the Alpha. The Omicron BA.1 did not have any statistical difference in the binding and neutralizing capability/activity so as in the case of Beta vs Kappa and Gamma vs Kappa (Figure 1A). In addition, based on the full-length spike, the Omicron BA.3 variant has the least binding and neutralizing capability/activity when compared with the wild-type (Figure 1B).

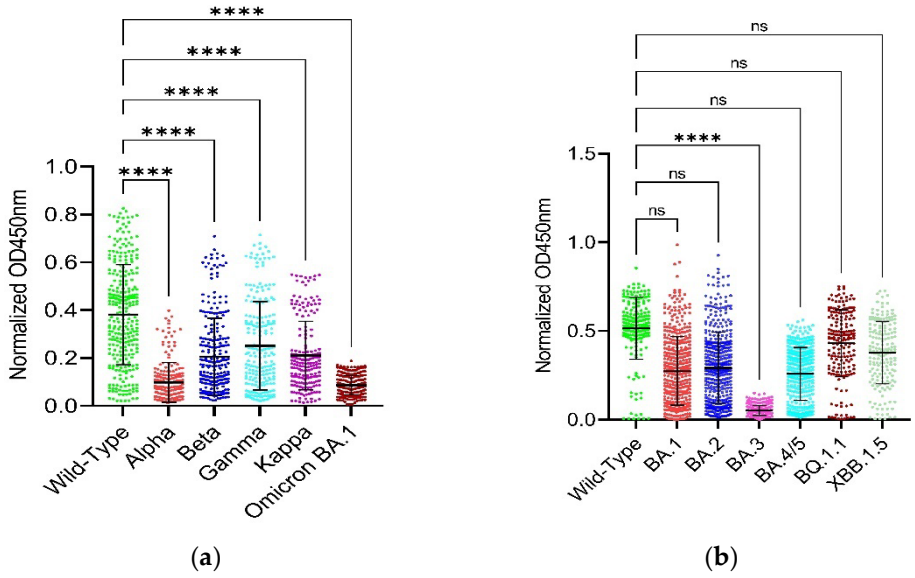

(**a**) (**b**)

Figure 1. Checking the neutralizing/binding activity/capability by normalized OD450nm values.

Figure 1A,B present the binding data using the RBD constructs. The results show that the Omicron BA.1 variant has the lowest binding capability (indicated by the lowest OD450nm values) in comparison with the wild-type Wuhan strain followed by Alpha, Kappa, Beta and Gamma variants with decreasing level of binding capability. On the other hand, Figure 1A,B also present the binding data using the full-length spike constructs. Here, the Omicron BA.3 variant displayed the lowest binding capability compared to the wild-type Wuhan strain, with a statistically significant difference ($p<0.0001$). The other Omicron variants (BA.1, BA.2, BA.4/5) did not show a statistically significant difference in binding capability compared to the wild-type when using the full-length spike. Figure 2A,B corroborate these findings from Figure 1A,B.

 doi:10.20944/preprints202405.1313.v1

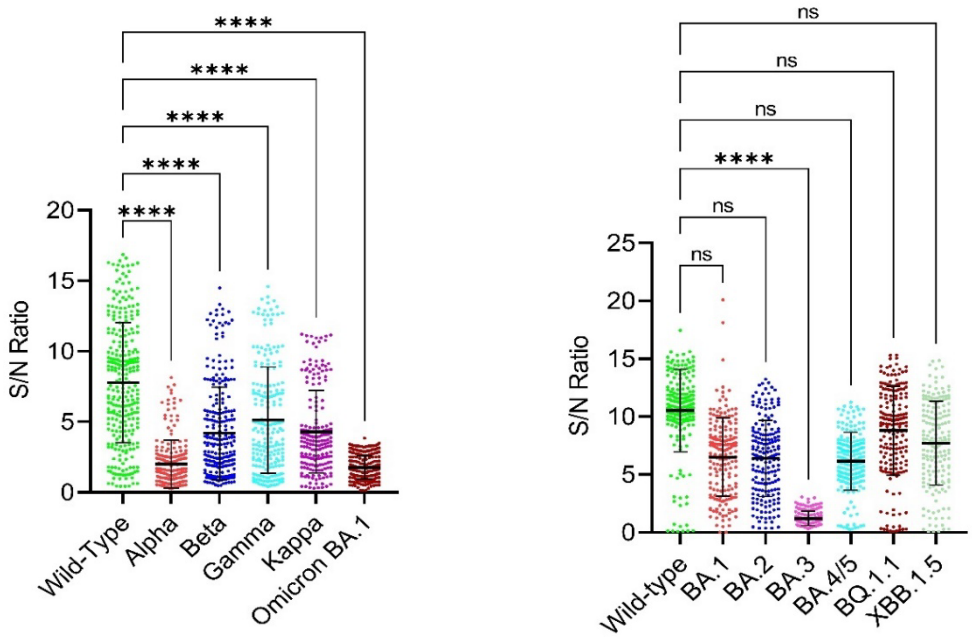

(**a**) (**b**)

Figure 2. Checking the neutralizing/binding activity/capability by S/N ratios. Figure 2 shows the confirmation of binding of serum antibodies from SARS-CoV-2-Wuhan convalescent patients with the RBD and full-length spike proteins of the SARS-CoV-2-Wuhan strain (i.e., RBD-WT) and the SARS-CoV-2-Omicron variants (full-length spike) has been checked by an indirect ELISA and compared by plotting a graph of S/N ratios measured on Y-axis and the SARS-CoV-2 variants on X-axis by applying appropriate statistical tests using GraphPad Prism version 9.5.1 software. Multiplicity adjusted P values are shown as follows: ns: $P > 0.05$, *$P \leq 0.05$, **$P \leq 0.01$, ***$P \leq 0.001$, ****$P \leq 0.0001$. Error bars indicate mean ± standard deviation. Each colored dot represents an individual S/N ratio for each individual serum sample for their respective variant. Error bars indicate mean ± standard error of mean (SEM). (**a**) It shows the S/N ratios on Y-axis and the RBD of wild-type, alpha, beta, gamma, kappa and Omicron BA.1 variants on X-axis. The data was analyzed by Kruskal-Wallis with Dunnett's T3 multiple Comparison test. (**b**) It shows the S/N ratios on Y-axis and the full-length spike of wild-type and Omicron BA.1, BA.2, BA.3, BA.4/5, BQ.1.1 and XBB.1.5 variants. The data was analyzed using the Welch's one-way ANOVA with Dunnett's T3 multiple Comparison test.

3.3. Comparison of Binding Capability between the RBD and Full-Length Spike of SARS-CoV-2 Wild-Type

Welch's unpaired t-test was used to compare the binding capability between the RBD and full-length spike of SARS-CoV-2 wild-type.

Although the RBD is the primary epitope compared to other part in spike protein, our graph shows that most of the serum samples have certainly higher binding capability as indicated by the overall higher normalized OD450nm values of the full-length spike protein of SARS-CoV-2 wild-type in comparison to that of the RBD but a few sera have the opposite results (Figure 3A,B).

 doi:10.20944/preprints202405.1313.v1

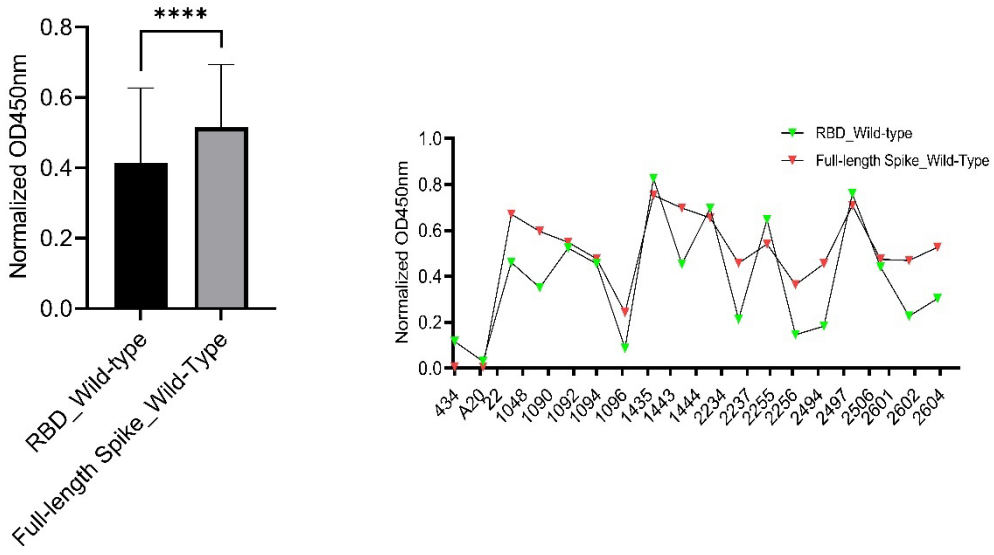

(**a**) (**b**)

Figure 3. Comparison of RBD and full-length Spike of wild-type SARS-CoV-2. Figure 3 shows comparison of the RBD and full-length spike of SARS-CoV-2 wild-type. The data was analyzed using Welch's unpaired t-test. Error bars indicate mean ± standard error of mean (SEM). Multiplicity adjusted P-value was shown as: ****P ≤ 0.0001 The data was analyzed by GraphPad Prism 9.5.1 software. (a) It shows the overall comparison. It shows that the full-length spike has overall higher normalized OD450nm values indicating the stronger binding of the full-length spike in comparison with its RBD domain (b) It shows the comparison with respect to individual serum sample. It shows that for some serum samples, the normalized OD450nm values of the full-length spike were higher than that of the RBD and vice versa.

3.4. Reduction Rates

The reduction rate of negative numbers means similar full-length spike binding capability of the serum sample to the SARS CoV-2 wild-type.

The reduction rate is calculated as (Normalized OD450 nm of wild type—Normalized OD450nm of the respective variant)/ (Normalized OD450nm of wild type) × 100.

For some sera, the reduction rates could not be calculated because of the less quantity of the sera. The reduction rates with negatives means similar RBD binding capability of the serum samples to the wild-type SARS-CoV-2. The data was analyzed using Brown-Forsythe and Welch ANOVA with Dunnett's T3 multiple comparison test and 95% confidence interval using GraphPad Prism version 9.5.1 software. The OD450 values were normalized by subtracting each sample value from that of the blank wells.

The convalescent serum antibodies indicate a significantly higher reduction in binding to the Omicron variant of SARS-CoV-2 which goes up to 96% reduction compared to the wild-type SARS-CoV-2 (Table 3, Figure 4A). The reduction in binding activity is statistically non-significant in comparison to the Alpha variant with average reduction rate of 72.79% but is significant in comparison to the Beta, Gamma, and Kappa variants for which the average reduction rate is 44.70, 36.49 and 50.23% respectively.

Table 3. Reduction rates based on RBD.

Sample ID	Wild-type	Alpha	Beta	Gamma	Kappa	Omicron BA.1	Alpha	Beta	Gamma	Kappa	Omicron BA.1
	Normalized OD450nm						% Reduction rate				
Y1	0.5906					0.0217					96.3241
Y3	0.5516					0.0327					94.0699
Y6	0.6169					0.0260					95.7786
Y11	0.6216					0.0387					93.7724

 doi:10.20944/preprints202405.1313.v1

Y14	0.0772					0.0080					89.5870
Y17	0.0712	0.0185	0.0429	0.0633	0.0499	0.0767	74.0250	39.7036	11.0764	29.8947	-7.7028
Y18	0.6452					0.0244					96.2223
Y20	0.4822	0.0825	0.2151	0.2907	0.2029	0.1307	82.8917	55.3917	39.7235	57.9176	72.8946
434	0.0743	0.0365	0.0627	0.0598	0.0564	0.0697	50.8754	15.7011	19.5872	24.1833	6.2286
A20	0.0372	0.0200	0.0358	0.0320	0.0307	0.0364	46.3758	3.8943	14.0421	17.5490	2.2900
32	0.4472	0.0708	0.2168	0.2827	0.1998		84.1615	51.5280	36.7950	55.3323	
22	0.3422	0.1392	0.1734	0.2278	0.1814	0.0809	59.3188	49.3190	33.4264	46.9854	76.3518
1048	0.3469	0.0649	0.1329	0.1356	0.1050	0.0818	81.3050	61.6918	60.9231	69.7234	76.4137
1090	0.5393	0.1511	0.4273	0.3681	0.2831	0.1146	71.9890	20.7672	31.7477	47.5026	78.7523
1092	0.6090	0.2219	0.4743	0.3924	0.3439	0.1232	63.5714	22.1134	35.5598	43.5281	79.7780
1094	0.3238	0.0967	0.1162	0.1201	0.1000	0.0527	70.1217	64.1049	62.9038	69.1065	83.7211
1096	0.1120	0.0302	0.0557	0.0780	0.0618	0.0675	73.0502	50.3000	30.3604	44.8563	39.7474
1435	0.6398	0.2261	0.5523	0.5703	0.4649	0.1504	64.6668	13.6773	10.8552	27.3300	76.4959
1443	0.4051	0.0876	0.1973	0.2662	0.1593	0.0928	78.3876	51.3034	34.2987	60.6869	77.0882
1444	0.6337	0.1072	0.2221	0.2755	0.1893	0.1025	83.0806	64.9513	56.5267	70.1346	83.8257
2234	0.2787	0.0811	0.1219	0.1707	0.1423	0.0763	70.9189	56.2687	38.7682	48.9585	72.6131
2237	0.7146	0.2917	0.4901	0.5675	0.4804	0.1592	59.1743	31.4104	20.5800	32.7651	77.7251
2255	0.5131	0.1106	0.1944	0.2577	0.2131	0.0825	78.4515	62.1007	49.7780	58.4651	83.9226
2256	0.2202	0.0345	0.0851	0.1022	0.0756	0.0652	84.3262	61.3536	53.6091	65.6735	70.4161
2494	0.3659	0.0601	0.1266	0.1683	0.1196	0.0843	83.5864	65.3963	53.9933	67.3132	76.9511
2497	0.7069	0.1897	0.4673	0.5163	0.4076	0.1543	73.1610	33.8966	26.9569	42.3393	78.1672
2506	0.4711	0.0977	0.2163	0.2747	0.1899	0.0740	79.2546	54.0866	41.6912	59.6798	84.2906
2601	0.2567	0.0452	0.0868	0.1167	0.0849	0.0612	82.3848	66.1978	54.5553	66.9173	76.1740
2602	0.3916	0.0919	0.1969	0.2517	0.1704	0.1588	76.5323	49.7020	35.7264	56.4735	59.4353
2604	0.5237	0.1294	0.3768	0.4072	0.3023	0.1483	75.2944	28.0577	22.2552	42.2855	71.6771

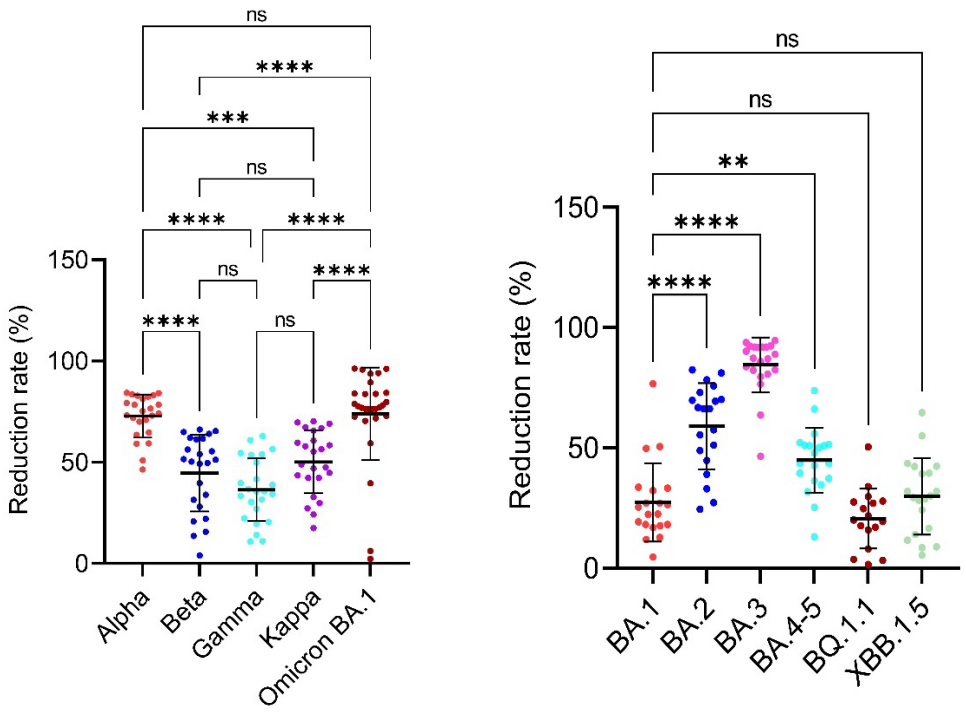

(**a**) (**b**)

Figure 4. Reduction rates. Figure 4 shows the percentage (%) reduction rates of the respective SARS-CoV-2 variants in comparison to the wild-type strain to check the neutralization or binding activity/capability of each respective variant against the convalescent serum IgG antibodies. Each colored dot represents an individual reduction rate for each individual serum sample for their respective variant. Multiplicity adjusted P values are shown as follows: ns: $P > 0.05$, *$P \leq 0.05$, **$P \leq 0.01$, ***$P \leq 0.001$, ****$P \leq 0.0001$. Error bars indicate mean ± standard deviation. The data was analyzed by GraphPad Prism 9.5.1 software. The higher reduction rate indicates the lower binding capability or neutralization activity. (a) It shows reduction rates on Y-axis based on the RBD of alpha, beta,

 doi:10.20944/preprints202405.1313.v1

gamma, kappa and Omicron BA.1 on X-axis and the data was analyzed by the Kruskal-Wallis with Dunnett's T3 multiple Comparison test. (b) It shows reduction rates on Y-axis based on the full-length spike of Omicron BA.1, BA.2, BA.3, BA.4/5, BQ.1.1 and XBB.1.5 on X-axis and the data was analyzed by the Welch's one-way ANOVA with Dunnett's T3 multiple.

The convalescent serum antibodies indicate significantly higher reduction in binding to the BA.3 Omicron SARS-CoV-2 variant which goes up to 84.56% followed by Omicron, Alpha, Omicron BA.2, Kappa, Omicron BA.4/5, Beta, Gamma, XBB.1.5, BA.1 and BQ.1.1 Omicron when compared to the wild-type SARS-CoV-2 with average reduction rates of 73.95, 59.07, 50.23, 44.91, 44.70, 36.48, 29.84, 27.34 and 20.59% respectively (Table 4, Figures 4B and 5).

Table 4. Reduction rates based on full-length spike.

Sample ID	Wild-type	BA.1	BA.2	BA.3	BA.4/5	BQ.1.1	XBB.1.5	BA.1	BA.2	BA.3	BA.4/5	BQ.1.1	XBB.1.5
	Normalized OD450nm							% Reduction rate					
434	0.0543	0.05933	0.0623	0.0290	0.2110	0.0694	0.0453	-9.2062	-14.7278	46.6239	-288.3568	-27.7722	16.6151
A20	0.0570	0.03800	0.0430	0.0207	0.0280	0.0675	0.0432	33.3312	24.5590	63.7415	50.8756	-18.4805	24.2201
22	0.5859	0.13633	0.1580	0.0363	0.5093	0.4823	0.4137	76.7304	73.0323	93.7986	13.0663	17.6788	29.3808
1048	0.6076	0.44333	0.2013	0.0987	0.3160	0.4568	0.3500	27.0298	66.8616	83.7600	47.9881	24.8208	42.3967
1090	0.5864	0.51633	0.3577	0.0760	0.3997	0.5772	0.5364	11.9550	39.0108	87.0405	31.8490	1.5763	8.5306
1092	0.6096	0.50633	0.4430	0.1180	0.3980	0.5870	0.5385	16.9338	27.3239	80.6416	34.7063	3.7040	11.6523
1094	0.5342	0.35433	0.2383	0.0410	0.2363	0.3852	0.3230	33.6728	55.3867	92.3253	55.7611	27.8952	39.5435
1096	0.2888	0.14500	0.1227	0.0367	0.0757	0.1432	0.1019	49.7881	57.5219	87.3027	73.7974	50.4120	64.7270
1435	0.6120	0.50367	0.2990	0.0677	0.3897	0.6219	0.5784	17.7013	51.1436	88.9433	36.3288	-1.6122	5.4874
1443	0.6080	0.49733	0.2050	0.0493	0.3433	0.5112	0.4326	18.2015	66.2828	91.8859	43.5305	15.9211	28.8423
1444	0.6041	0.45067	0.2033	0.0483	0.3410	0.4869	0.4327	25.3998	66.3416	91.9992	43.5533	19.4078	28.3658
2234	0.5033	0.37033	0.1093	0.0493	0.2447	0.3648	0.2902	26.4236	78.2781	90.1986	51.3905	27.5321	42.3455
2237	0.5961	0.52000	0.3990	0.1047	0.3733	0.5481	0.5126	12.7677	33.0660	82.4417	37.3717	8.0559	14.0028
2255	0.5719	0.44367	0.1707	0.0807	0.2847	0.4572	0.4003	22.4206	70.1573	85.8947	50.2233	20.0544	30.0029
2256	0.5073	0.25100	0.0953	0.0410	0.1717	0.3351	0.2279	50.5254	81.2089	91.9185	66.1628	33.9510	55.0866
2494	0.5384	0.39300	0.1647	0.0407	0.2643	0.4463	0.3662	27.0117	69.4180	92.4474	50.9078	17.1110	31.9903
2497	0.6054	0.48833	0.3090	0.1420	0.3660	0.5858	0.5516	19.3428	48.9630	76.5461	39.5484	3.2520	8.8869
2506	0.5287	0.35800	0.1277	0.0433	0.2527	0.3858	0.3211	32.2822	75.8511	91.8032	52.2066	27.0324	39.2655
2601	0.4848	0.37567	0.0850	0.0260	0.2373	0.3401	0.2736	22.5072	82.4661	94.6367	51.0427	29.8465	43.5538
2602	0.5938	0.48567	0.1790	0.1050	0.3403	0.4641	0.4043	18.2071	69.8539	82.3166	42.6832	21.8414	31.9096
2604	0.6279	0.59867	0.3463	0.1283	0.4693	0.6625	0.6641	4.6538	44.8415	79.5611	25.2519	-5.5177	-5.7646

Preprints.org (www.preprints.org) | NOT PEER-REVIEWED | Posted: 21 May 2024 doi:10.20944/preprints202405.1313.v1

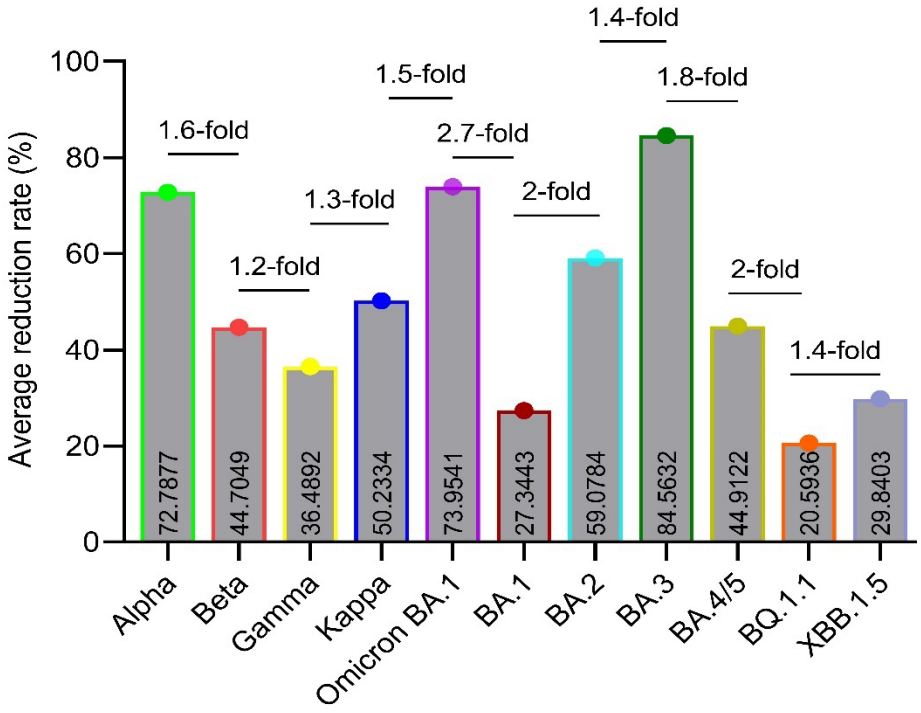

Figure 5. Average reduction rates (%) and fold-changes of average reduction rate. Figure 5 indicates the average reduction rates (%) along with the fold-changes in the average reduction rates on Y-axis in comparison to the Alpha and the SARS-CoV-2 variants on X-axis. The data was analyzed by GraphPad Prism 9.5.1 software. As the calculation of the reduction rate itself considers the wild-type variant that is why the wild-type has not been shown on the graph.

3.5. Figures and Tables

Figure 1 shows the binding of serum antibodies from SARS-CoV-2-Wuhan convalescent patients with the RBD and full-length spike proteins of the SARS-CoV-2-Wuhan strain (i.e., RBD-WT) and the SARS-CoV-2-Omicron variants (full-length spike) has been checked by an indirect ELISA and compared by plotting a graph of OD values measured at 450nm wavelength on Y-axis and the SARS-CoV-2 variants on X-axis by applying appropriate statistical tests using GraphPad Prism version 9.5.1 software. Multiplicity adjusted P values are shown as follows: ns: $P > 0.05$, *$P \leq 0.05$, **$P \leq 0.01$, ***$P \leq 0.001$, ****$P \leq 0.0001$. Error bars indicate mean ± standard deviation. Each colored dot represents an individual OD450nm value for each individual serum sample for their respective variant. The higher the normalized OD450nm values, the more the binding affinity of the serum antibodies with the respective protein of the respective variant (a) It shows the normalized OD450nm values on Y-axis and the RBD of wild-type, alpha, beta, gamma, kappa and Omicron BA.1 variants on X-axis. The data was analyzed by Kruskal-Wallis with Dunnett's T3 multiple Comparison test. (b) It shows the normalized OD450nm values on Y-axis and the full-length spike of wild-type and Omicron BA.1, BA.2, BA.3, BA.4/5, BQ.1.1 and XBB.1.5 variants. The data was analyzed using Welch's one-way ANOVA with Dunnett's T3 multiple Comparison test.

4. Discussion

The emergence of the Alpha, Beta, Gamma and Kappa SARS-CoV-2 variants during the early COVID-19 pandemic, and the BA.1, BA.2, BA.3, BA.4/5, BQ.1.1 and XBB.1.5 sub-lineages of the B.1.1.529 (Omicron) SARS-CoV-2 variants later during the pandemic has raised serious concerns regarding the longevity of infection- and vaccine-induced immunity in the face of the virus's ongoing evolution [12]. The RBD and full-length spike proteins of different variants of SARS-CoV-2 have been studied extensively to design and develop anti-SARS-CoV-2 vaccines using a more reasonable and

 doi:10.20944/preprints202405.1313.v1

appropriate approach. The immunoglobulin G (IgG) is one of the main indicators of the neutralizing activity in the blood so, in this study, the capability of the SARS-CoV-2 wild-type, Alpha, Beta, Gamma, Kappa, and the BA.1, BA.2, BA.3, BA.4/5, BQ.1.1 and XBB.1.5 Omicron variants to escape the convalescent serum IgG antibodies induced by natural infection of early original Wuhan strain was evaluated by the indirect ELISA method using the corresponding RBD and full-length spike as the coating antigens.

Based on the RBD of SARS-CoV-2, the Omicron BA.1 variant shows the lowest binding or neutralization and hence highest number of immune escape mutations followed by Alpha, Kappa, Beta and Gamma in comparison with the wild-type strain (Figure 1A,B). This lower binding and neutralization of the Omicron variant can be explained by the presence of more than 30 mutations which are thought to be responsible for their decreased neutralizing or binding activity/capability and hence increased antibody escape [13]. These results are consistent with those of the Chi and colleagues in 2022 who reported that the Omicron BA.1 had decreased neutralization capability and partially evaded the IgG and IgA antibodies produced after anti-SARS-CoV-2 vaccine's first dose [14].

The Alpha variant showed significantly lower neutralization in comparison with the wild-type strain and Beta variant (Figure 1A). These results are consistent with the previous studies [15,16]. Our study showed significantly reduced neutralizing activity of the Gamma variant in comparison with the wild-type Wuhan strain (Figure 1A). These results are consistent with the previous studies [17–20].

The BA.1, BA.2, BA.4/5, BQ.1.1 and XBB.1.5 Omicron variants did not show any statistical difference in comparison to the wild-type Wuhan strain indicating that the new anti-SARS-CoV-2 vaccines might not need to incorporate the Omicron variants other than BA.3 (Figure 1B). These results are not consistent with the study of Kurhade and colleagues conducted in late 2022 and published in 2023 in which they reported reduced neutralization and hence high immune evasion of BA.2.75.2, BQ.1.1 and XBB.1 Omicron variants as compared with the parental viral strain, XBB.1 showing the highest immune evasion potential [21]. Unlike the results of Wang and colleagues in 2023 who reported that in comparison to the wild-type Wuhan strain, the BA.2 and BA.4/5 had stronger immune evasion to the serum neutralization [22], our results showed that both the BA.2 and BA.4/5 had no significant difference in the serum neutralization in comparison with the wild-type Wuhan strain (Figure 1B).

In addition, our study reported that the currently circulating Omicron BQ.1.1 and XBB.1.5 variants did not have significant difference between their neutralization or binding activities/capabilities and per cent reduction between each other (Figure 1B). These results are not consistent with the previous study [23]. Our study also showed that the BA.1 and BA.2 Omicron variants did not have statistically significant difference between their S/N ratios but the reduction rate of BA.2 is 2.16-fold higher than that of the BA.1 (Figure 2B). The reason for this might be the shared 32 mutations among these variants [24]. Our results are consistent with the results of Yu and colleagues in 2022 [24]. The other results of S/N ratios are like that of the normalized OD450nm results (Figure 2A,B).

In terms of reduction rates in the binding capability and neutralization activity, more than 2-fold increase in the reduction rate is usually considered larger and less than 1.5-fold increase as smaller [25]. Our study showed that when compared with the Alpha variant, the Beta, Gamma, Kappa, Omicron BA.1 and the BA.1, BA.2, BA.3, BA.4/5, BQ.1.1 and XBB.1.5 Omicron variants have -1.6-, -1.9-, -1.5-, 1-, -2.6-, -1.2-, 1.1-, -1.6-, -3.5- and -2.4- fold change in the average reduction respectively (Figure 5). The study of Caniels and colleagues in 2021 reported that when compared with the wild-type, the Alpha, Beta and Gamma variants have -1.6,-, -3.6- and -2.8- fold reduction in the non-hospitalized and -0.5-, -7.1- and -3.8- fold lower reduction in the hospitalized convalescent patients [25]. In terms of reduction rates, the Beta variant shows an average reduction rate of 44.70% which is 1.6-fold (72.79/44.70 = 1.6) lower than that of the Alpha variant with an average reduction rate of 72.79% (Figure 5). These results are not consistent with the results of Wang and colleagues in 2021 [26].

Our study showed up to about 96% reduction with an average reduction of 73.95% in binding to the RBD of Omicron BA.1 variant in comparison to the wild-type Wuhan strain and the Alpha and Omicron BA.1 variants had no significant fold change ($P > 0.5$) (Figure 5). This data indicates that

 doi:10.20944/preprints202405.1313.v1

while developing anti-SARS-CoV-2 vaccines, either the Alpha or the Omicron BA.1 variant needs to be considered.

Our study showed that the convalescent serum IgG antibodies indicate the highest reduction rates up to about 94% reduction with an average of 84.56% in binding to the full-length spike of Omicron BA.3 variant in comparison to the wild-type Wuhan strain and this reduction is 1.1- (84.5632/73.9541), 3.1- (84.5632/27.3443), 1.4- (84.5632/59.0784), 1.8- (84.5632/44.9122), 4.1- (84.5632/20.5936) and 2.8- (84.5632/29.8403) fold increase when compared with the Omicron, BA.1, BA.2, BA.3, BA.4/5, BQ.1.1 and XBB.1.5 Omicron respectively (values not shown in Figure 5).

Also, in this study, the average reduction rates of the Beta, Kappa and Gamma variants were shown to be 44.7049, 36.4892 and 50.2334% in comparison with the wild-type Wuhan strain with fold change in the average reduction of -1.2 (44.7049/36.4892), 1.1 (50.2334/44.7049) and 1.37 (50.2334/36.4892) of Gamma in comparison to the Beta, Kappa in comparison to the Beta and Kappa in comparison to the Gamma which indicates that there is no significant difference between the Beta, Gamma, and Kappa variants. Hence, there is no need to consider these variants to design anti-SARS-CoV-2 vaccines.

Also, there is no statistical difference between the reduction rates of Beta/Gamma and Beta/Kappa and only a slight difference between Gamma/Kappa variants (Figure 4A). These results indicate and confirm that the Omicron variant probably has the highest number of immune escape mutations in its RBD protein when compared with the SARS-CoV-2 wild-type, Alpha, Beta, Gamma, and Kappa variants. In addition, in terms of the reduction rates based on their full-length spike, the Omicron BA.3 has overall the highest reduction rates up to about 94% and it is statistically significant in comparison to all the other Omicron variants of this study (Figure 4B). Also, there is only a slight difference in the reduction rates of BA.1 and BA.4/5 (**), and BA.4/5 and XBB.1.5 (*) and no statistically significant difference in the reduction rates of Omicron BA.1/BQ.1.1, BA.1/XBB.1.5 and BQ.1.1/XBB.1.5 variants (Figure 4B) which means that the Omicron BA.3 variant probably has some unique mutations which help it to escape from the immune system and the lack of/less statistical differences between the other variants show that there is no significant need to consider those variants while designing new anti-SARS-CoV-2 vaccines and the inactivated anti-SARS-CoV-2 vaccine using only the original Wuhan or wild-type strain is sufficient to cope with even the latest Omicron infections as checked by the indirect ELISA alone.

ELISA has some advantages over virus neutralization test (VNT) as ELISA is simpler, faster, less labor-intensive and does not require BSL-3 facility [27]. Also, Vilibic-Cavlek and colleagues have reported that the results of ELISA and VNT are comparable [28]. Our study encountered some challenges. Firstly, we had a limited number of serum samples available at the initial phase of the COVID-19 pandemic. Secondly, although we assessed neutralization and binding capability/activity using ELISA, it would have been ideal to confirm these findings using a pseudo- or actual- SARS-CoV-2 virus neutralization test but due to limited access to a biosafety level-3 (BSL-3) facility and serum consumption, this was not feasible. Also, another limitation might be that the SARS-CoV-2 variants are mutating so rapidly that some recent research papers may not be cited in a timely manner.

5. Conclusions

From our study, it is concluded that there is a need to study the immune evasion of the currently circulating SARS-CoV-2 variants which could render the current anti-SARS-CoV-2 vaccines ineffective. It has been shown in this study that there is a need to consider the Alpha, Beta, Gamma, Kappa, Omicron BA.1 and the BA.3 Omicron variants as the IgG antibodies of the convalescent sera showed reduced neutralization activity Because the iELISA could not always distinguish the binding of neutralizing epitopes from other epitopes, other omicron variants like XBB.1.5 may still show the immune escape to Wuhan convalescent patients though these sera show binding potential. Therefore, vaccines against Omicron XBB.1.5 variant and others might still be needed. This study helps us to better understand the immune evasion of the earlier and the currently circulating variants of SARS-

 doi:10.20944/preprints202405.1313.v1

CoV-2. This study will help the scientific community and vaccine production industry in better and more informed vaccine design strategies based on the immune evasion of the target variants.

Supplementary Materials: The following supporting information can be downloaded at the website of this paper posted on Preprints.org.

Author Contributions: Conceptualization, Behzad Hussain, Peizhe Zhao and Bo Yang; Formal analysis, Behzad Hussain; Methodology, Behzad Hussain, Xiaoxiong Li and Zhichao Zhang; Resources, Peizhe Zhao and Bo Yang; Supervision, Demei Zhang, Defen Lu and Wu Changxin; Visualization, Behzad Hussain; Writing—original draft, Behzad Hussain; Writing—review & editing, Behzad Hussain, Xiaoxiong Li, Zhichao Zhang, Guoqiang Feng, Demei Zhang and Defen Lu. All the authors contributed and approved the submitted version of this article. All authors have read and agreed to the published version of the manuscript.

Funding: This work was supported by the National Key R&D Program of China (2021YFC2301400), the Science and Technology Major Projects of Shanxi Province (Grant 202005D121008), Shanxi Provincial Key R&D Project (202003D31005/GZ), Transformation of Scientific and Technological Achievements Programs of Higher Education Institutions in Shanxi (TSTAP) and Shanxi Provincial Key Laboratory for Major Infectious Disease Response.

Institutional Review Board Statement: The study was conducted according to the guidelines of the Declaration of Helsinki and approved by the Shanxi University Ethical Committee.

Informed Consent Statement: Informed consent was obtained from all subjects involved in the study.

Conflicts of Interest: The authors declare no conflict of interest.

References

1. Cucinotta, D.; Vanelli, M.J.A.b.m.A.p. WHO declares COVID-19 a pandemic. 2020, 91, 157.
2. Jeyanathan, M.; Afkhami, S.; Smaill, F.; Miller, M.S.; Lichty, B.D.; Xing, Z.J.N.R.I. Immunological considerations for COVID-19 vaccine strategies. 2020, 20, 615-632.
3. Hoffmann, M.; Arora, P.; Groß, R.; Seidel, A.; Hörnich, B.F.; Hahn, A.S.; Krüger, N.; Graichen, L.; Hofmann-Winkler, H.; Kempf, A.J.C. SARS-CoV-2 variants B. 1.351 and P. 1 escape from neutralizing antibodies. 2021, 184, 2384-2393. e2312.
4. Norman, M.; Gilboa, T.; Ogata, A.F.; Maley, A.M.; Cohen, L.; Busch, E.L.; Lazarovits, R.; Mao, C.-P.; Cai, Y.; Zhang, J.J.N.B.E. Ultrasensitive high-resolution profiling of early seroconversion in patients with COVID-19. 2020, 4, 1180-1187.
5. Krammer, F.; Simon, V.J.S. Serology assays to manage COVID-19. 2020, 368, 1060-1061.
6. Esposito, D.; Mehalko, J.; Drew, M.; Snead, K.; Wall, V.; Taylor, T.; Frank, P.; Denson, J.-P.; Hong, M.; Gulten, G.J.P.e.; et al. Optimizing high-yield production of SARS-CoV-2 soluble spike trimers for serology assays. 2020, 174, 105686.
7. Gribble, J.; Stevens, L.J.; Agostini, M.L.; Anderson-Daniels, J.; Chappell, J.D.; Lu, X.; Pruijssers, A.J.; Routh, A.L.; Denison, M.R.J.P.p. The coronavirus proofreading exoribonuclease mediates extensive viral recombination. 2021, 17, e1009226.
8. Korber, B.; Fischer, W.M.; Gnanakaran, S.; Yoon, H.; Theiler, J.; Abfalterer, W.; Hengartner, N.; Giorgi, E.E.; Bhattacharya, T.; Foley, B.J.C. Tracking changes in SARS-CoV-2 spike: evidence that D614G increases infectivity of the COVID-19 virus. 2020, 182, 812-827. e819.
9. O'Toole, Á.; Scher, E.; Underwood, A.; Jackson, B.; Hill, V.; McCrone, J.T.; Colquhoun, R.; Ruis, C.; Abu-Dahab, K.; Taylor, B.J.V.e. Assignment of epidemiological lineages in an emerging pandemic using the pangolin tool. 2021, 7, veab064.
10. Control, C.f.D.; Prevention. SARS-CoV-2 variant classifications and definitions. 2021.
11. SARS-CoV, C. Variant classifications and definitions.
12. Evans, J.P.; Qu, P.; Zeng, C.; Zheng, Y.-M.; Carlin, C.; Bednash, J.S.; Lozanski, G.; Mallampalli, R.K.; Saif, L.J.; Oltz, E.M.J.N.E.J.o.M. Neutralization of the SARS-CoV-2 deltacron and BA. 3 variants. 2022, 386, 2340-2342.
13. Harvey, W.T.; Carabelli, A.M.; Jackson, B.; Gupta, R.K.; Thomson, E.C.; Harrison, E.M.; Ludden, C.; Reeve, R.; Rambaut, A.; Microbiology, C.-G.U.C.J.N.R. SARS-CoV-2 variants, spike mutations and immune escape. 2021, 19, 409-424.

 doi:10.20944/preprints202405.1313.v1

14. Chi, X.; Guo, Y.; Zhang, G.; Sun, H.; Zhang, J.; Li, M.; Chen, Z.; Han, J.; Zhang, Y.; Zhang, X.J.S.T.; et al. Broadly neutralizing antibodies against Omicron-included SARS-CoV-2 variants induced by vaccination. 2022, 7, 139.
15. Maeda, K.; Amano, M.; Uemura, Y.; Tsuchiya, K.; Matsushima, T.; Noda, K.; Shimizu, Y.; Fujiwara, A.; Takamatsu, Y.; Ichikawa, Y.J.S.R. Correlates of neutralizing/SARS-CoV-2-S1-binding antibody response with adverse effects and immune kinetics in BNT162b2-vaccinated individuals. 2021, 11, 22848.
16. Tsuchiya, K.; Maeda, K.; Matsuda, K.; Takamatsu, Y.; Kinoshita, N.; Kutsuna, S.; Hayashida, T.; Gatanaga, H.; Ohmagari, N.; Oka, S.J.S.R. Neutralization activity of IgG antibody in COVID-19-convalescent plasma against SARS-CoV-2 variants. 2023, 13, 1263.
17. Wall, E.C.; Wu, M.; Harvey, R.; Kelly, G.; Warchal, S.; Sawyer, C.; Daniels, R.; Hobson, P.; Hatipoglu, E.; Ngai, Y.J.T.L. Neutralising antibody activity against SARS-CoV-2 VOCs B. 1.617. 2 and B. 1.351 by BNT162b2 vaccination. 2021, 397, 2331-2333.
18. Faria, N.R.; Mellan, T.A.; Whittaker, C.; Claro, I.M.; Candido, D.d.S.; Mishra, S.; Crispim, M.A.; Sales, F.C.; Hawryluk, I.; McCrone, J.T.J.S. Genomics and epidemiology of the P. 1 SARS-CoV-2 lineage in Manaus, Brazil. 2021, 372, 815-821.
19. Wang, P.; Casner, R.G.; Nair, M.S.; Wang, M.; Yu, J.; Cerutti, G.; Liu, L.; Kwong, P.D.; Huang, Y.; Shapiro, L.J.C.h.; et al. Increased resistance of SARS-CoV-2 variant P. 1 to antibody neutralization. 2021, 29, 747-751. e744.
20. Garcia-Beltran, W.F.; Lam, E.C.; Denis, K.S.; Nitido, A.D.; Garcia, Z.H.; Hauser, B.M.; Feldman, J.; Pavlovic, M.N.; Gregory, D.J.; Poznansky, M.C.J.C. Multiple SARS-CoV-2 variants escape neutralization by vaccine-induced humoral immunity. 2021, 184, 2372-2383. e2379.
21. Kurhade, C.; Zou, J.; Xia, H.; Liu, M.; Chang, H.C.; Ren, P.; Xie, X.; Shi, P.Y.J.N.m. Low neutralization of SARS-CoV-2 Omicron BA. 2.75. 2, BQ. 1.1 and XBB. 1 by parental mRNA vaccine or a BA. 5 bivalent booster. 2023, 29, 344-347.
22. Wang, Q.; Iketani, S.; Li, Z.; Liu, L.; Guo, Y.; Huang, Y.; Bowen, A.D.; Liu, M.; Wang, M.; Yu, J.J.C. Alarming antibody evasion properties of rising SARS-CoV-2 BQ and XBB subvariants. 2023, 186, 279-286. e278.
23. Yue, C.; Song, W.; Wang, L.; Jian, F.; Chen, X.; Gao, F.; Shen, Z.; Wang, Y.; Wang, X.; Cao, Y.J.T.L.I.D. ACE2 binding and antibody evasion in enhanced transmissibility of XBB. 1.5. 2023, 23, 278-280.
24. Yu, J.; Collier, A.-r.Y.; Rowe, M.; Mardas, F.; Ventura, J.D.; Wan, H.; Miller, J.; Powers, O.; Chung, B.; Siamatu, M.J.N.E.J.o.M. Neutralization of the SARS-CoV-2 Omicron BA. 1 and BA. 2 variants. 2022, 386, 1579-1580.
25. Caniels, T.G.; Bontjer, I.; van der Straten, K.; Poniman, M.; Burger, J.A.; Appelman, B.; Lavell, A.A.; Oomen, M.; Godeke, G.-J.; Valle, C.J.S.A. Emerging SARS-CoV-2 variants of concern evade humoral immune responses from infection and vaccination. 2021, 7, eabj5365.
26. Wang, P.; Nair, M.S.; Liu, L.; Iketani, S.; Luo, Y.; Guo, Y.; Wang, M.; Yu, J.; Zhang, B.; Kwong, P.D.J.N. Antibody resistance of SARS-CoV-2 variants B. 1.351 and B. 1.1. 7. 2021, 593, 130-135.
27. Adams, O.; Andrée, M.; Hermsen, D.; Lübke, N.; Timm, J.; Schaal, H.; Müller, L.J.J.o.V.M. Comparison of commercial SARS-CoV-2 surrogate neutralization assays with a full virus endpoint dilution neutralization test in two different cohorts. 2022, 307, 114569.
28. Vilibic-Cavlek, T.; Bogdanic, M.; Borko, E.; Hruskar, Z.; Zilic, D.; Ferenc, T.; Tabain, I.; Barbic, L.; Vujica Ferenc, M.; Ferencak, I.J.A. Detection of SARS-CoV-2 Antibodies: Comparison of Enzyme Immunoassay, Surrogate Neutralization and Virus Neutralization Test. 2023, 12, 35.
29. O'Toole, Á.; Hill, V.; Pybus, O.G.; Watts, A.; Bogoch, I.I.; Khan, K.; Messina, J.P.; COVID, T.; Network, B.-U.C.G.; Tegally, H.J.W.O.R. Tracking the international spread of SARS-CoV-2 lineages B. 1.1. 7 and B. 1.351/501Y-V2 with grinch. 2021, 6.
30. Tulimilli, S.V.; Dallavalasa, S.; Basavaraju, C.G.; Kumar Rao, V.; Chikkahonnaiah, P.; Madhunapantula, S.V.; Veeranna, R.P.J.V. Variants of Severe Acute Respiratory Syndrome Coronavirus 2 (SARS-CoV-2) and Vaccine Effectiveness. 2022, 10, 1751.
31. Saxena, S.K.; Kumar, S.; Ansari, S.; Paweska, J.T.; Maurya, V.K.; Tripathi, A.K.; Abdel-Moneim, A.S.J.J.o.m.v. Characterization of the novel SARS-CoV-2 Omicron (B. 1.1. 529) variant of concern and its global perspective. 2022, 94, 1738-1744.
32. Karim, S.S.A.; Karim, Q.A.J.T.l. Omicron SARS-CoV-2 variant: a new chapter in the COVID-19 pandemic. 2021, 398, 2126-2128.

 doi:10.20944/preprints202405.1313.v1

33. Viana, R.; Moyo, S.; Amoako, D.G.; Tegally, H.; Scheepers, C.; Althaus, C.L.; Anyaneji, U.J.; Bester, P.A.; Boni, M.F.; Chand, M.J.N. Rapid epidemic expansion of the SARS-CoV-2 Omicron variant in southern Africa. 2022, 603, 679-686.
34. Tegally, H.; Moir, M.; Everatt, J.; Giovanetti, M.; Scheepers, C.; Wilkinson, E.; Subramoney, K.; Makatini, Z.; Moyo, S.; Amoako, D.G.J.N.m. Emergence of SARS-CoV-2 omicron lineages BA. 4 and BA. 5 in South Africa. 2022, 28, 1785-1790.
35. Islam, M.R.; Shahriar, M.; Bhuiyan, M.A.J.H.s.r. The latest Omicron BA. 4 and BA. 5 lineages are frowning toward COVID-19 preventive measures: a threat to global public health. 2022, 5.
36. Qu, P.; Evans, J.P.; Faraone, J.N.; Zheng, Y.-M.; Carlin, C.; Anghelina, M.; Stevens, P.; Fernandez, S.; Jones, D.; Lozanski, G.J.C.h.; et al. Enhanced neutralization resistance of SARS-CoV-2 omicron subvariants BQ. 1, BQ. 1.1, BA. 4.6, BF. 7, and BA. 2.75. 2. 2023, 31, 9-17. e13.
37. Kamp, J.; Abbott, B.J.W.S.J.-O.E. New Covid-19 Subvariant, XBB. 1.5, Takes Over in Parts of US. 2023, N. PAG-N. PAG.